J|A|C|S ARTICLES

Published on Web 07/01/2009

Fluorescent Single-Walled Carbon Nanotubes Following the 1,3-Dipolar Cycloaddition of Pyridinium Ylides

Mustafa K. Bayazit and Karl S. Coleman*

Department of Chemistry, Durham University, South Road, Durham DH1 3LE, United Kingdom

Received May 7, 2009; E-mail: k.s.coleman@durham.ac.uk

Abstract: Pyridinium ylides generated from simple Kröhnke salts undergo a 1,3-dipolar cycloaddition to single-walled carbon nanotubes (SWNTs) offering a simple and convenient method for the covalent modification of carbon nanotubes. The indolizine functionalized SWNTs generated, emit blue light when excited at 335 nm. The location and distribution of the functional groups was determined by AFM using electrostatic interactions with gold nanoparticles. While resonance Raman spectroscopy showed that the 1,3-dipolar cylcloaddition of the pyridinium ylides to the nanotube surface was selective for metallic and large diameter semiconducting SWNTs. The indolizine functionalized SWNTs were further characterized using FTIR, UV−vis-NIR, TGA−MS, and XPS.

Introduction

Carbon nanotubes (CNTs) have impressive electrical, thermal, and mechanical properties and many potential applications ranging from composite materials, energy storage, sensors, and field emission devices to nanoscale electronic components have been envisaged.[1,2] Unfortunately, due to strong intertube van der Waals forces CNTs, in particular single-walled carbon nanotubes (SWNTs), have a tendency to aggregate together into bundles, resulting in low solubility in both aqueous and nonaqueous solvents, making their handling and processing difficult. For this reason, much effort has been spent on introducing organic and inorganic functional groups to the surface of nanotubes to improve solubility and or provide a site for attachment of polymers, biomolecules, or other material. We have recently shown that the simple addition of tertiary phosphines to SWNTS can improve the solubility of the nanotubes in common organic solvents.[3] Noncovalent modification of CNTs, often resulting in increased solubility, can be achieved by using surfactants,[4] polymer wrapping[5,6] or by π-stacking of pyrenes, or other polycyclic aromatic compounds, onto the nanotube surface.[7−11] Whereas, covalently, strategies to improve solubility and to introduce functional groups to the nanotube surface have included radical,[12,13] cycloaddition,[14,15] and oxidation reactions.[16,17] The chemical modification of CNTs has been extensively reviewed.[18]

One of the most versatile routes to the covalent chemical modification of carbon nanotubes is perhaps 1,3-dipolar cycloadditions. In particular, the cycloaddition of azomethine ylides pioneered by Prato.[19] The reactive azomethine ylides used are typically generated in situ by decarboxylation of immonium salts derived from the thermal condensation of glycines with aldehydes,[20] or to a lesser extent by thermal ring-opening of aziridines.[21] The introduction of pyrrolidines to the surface of CNTs has been used extensively to aid in the transfection of CNTs into mammalian cells and for the delivery of pharmacologically active molecules such as peptides, MTX, and ampho-

(1) *Carbon Nanotubes: Synthesis, Structure, Properties and Applications*; Dresselhaus, M. S.; Dresselhaus, G.; Avouris, Ph., Eds.; Springer: Berlin, 2001.
(2) Rao, C. N. R.; Govindaraj, A.; *Nanotubes and Nanowires*; RSC Publishing: Cambridge, 2005.
(3) Suri, A.; Chakraborty, A. K.; Coleman, K. S. *Chem. Mater.* **2008**, *20*, 1705.
(4) Moore, V. C.; Strano, M. S.; Haroz, E. H.; Hague, R. H.; Smalley, R. E. *Nano Lett.* **2003**, *3*, 1379.
(5) O'Connell, M. J.; Boul, P.; Ericson, L. M.; Huffman, C.; Wang, Y.; Haroz, E.; Kuper, C.; Tour, J. M.; Ausman, K. D.; Smalley, R. E. *Chem. Phys. Lett.* **2001**, *342*, 265.
(6) Liu, A. H.; Honma, I.; Ichihara, M.; Zhou, H. S. *Nanotechnology* **2006**, *17*, 2845.
(7) Tomonari, Y.; Murakami, H.; Nakashima, N. *Chem.−Eur. J.* **2006**, *12*, 4027.
(8) Paloniemi, H.; Ääritalo, T.; Laiho, T.; Liuke, H.; Kocharova, N.; Haapakka, K.; Terzi, F.; Seeber, R.; Lukkari, J. *J. Phys. Chem. B* **2005**, *109*, 8634.
(9) Chen, R. J.; Zhang, Y.; Wang, D.; Dai, H. *J. Am. Chem. Soc.* **2001**, *123*, 3838.
(10) Star, A.; Liu, Y.; Grant, K.; Ridvan, L.; Stoddart, J. F.; Steuerman, D. W.; Diehl, M. R.; Boukai, A.; Heath, J. R. *Macromolecules* **2003**, *36*, 553.
(11) Yuan, W. Z.; Sun, J. Z.; Dong, Y. Q.; Haussler, M.; Yang, F.; Xu, H. P.; Qin, A. J.; Lam, J. W. Y.; Zheng, Q.; Tang, B. Z. *Macromolecules* **2006**, *39*, 8011.
(12) Price, B. K.; Tour, J. M. *J. Am. Chem. Soc.* **2006**, *128*, 12899.
(13) Hu, H.; Zhao, B.; Hamon, M. A.; Kamaras, K.; Itkis, M. E.; Haddon, R. C. *J. Am. Chem. Soc.* **2003**, *125*, 14893.
(14) Tagmatarchis, N.; Prato, M. *J. Mater. Chem.* **2004**, *14*, 437.
(15) Azamian, B. R.; Coleman, K. S.; Davis, J. J.; Hanson, N.; Green, M. L. H. *Chem. Commun.* **2002**, 366.
(16) Coleman, K. S.; Bailey, S. R.; Fogden, S.; Green, M. L. H. *J. Am. Chem. Soc.* **2003**, *125*, 8722.
(17) Coleman, K. S.; Chakraborty, A. K.; Bailey, S. R.; Sloan, J.; Alexander, M. *Chem. Mater.* **2007**, *19*, 1076.
(18) Tasis, D.; Tagmatarchis, N.; Bianco, A.; Prato, M. *Chem. Rev.* **2006**, *106*, 1105.
(19) Georgakilas, V.; Kordatos, K.; Prato, M.; Guldi, D. M.; Holzinger, M.; Hirsch, A. *J. Am. Chem. Soc.* **2002**, *124*, 760.
(20) Tagmatarchis, N.; Prato, M. *J. Mater. Chem.* **2004**, *14*, 437.
(21) Brunetti, F. G.; Herrero, M. A.; de, M./initials>; Muoz, J.; Giordani, S.; Daz-Ortiz, A.; Filippone, S.; Ruaro, G; Meneghetti, M.; Prato, M.; Vzquez, E. *J. Am. Chem. Soc.* **2007**, *129*, 14580.

10.1021/ja903712f CCC: $40.75

tericin B.[22,23] Other 1,3-dipolar cycloaddition reactions to carbon nanotubes have involved ozone,[24,25] nitrile imines,[26] and nitrile oxides.[27]

Although the derivativization of CNTs is highly desirable, the challenge remains to achieve sufficient functionalization of the CNT surface to ensure ease of processing or facilitate the attachment of active molecules or particles, while avoiding significant degradation of the structure which could compromise the exciting properties of the material.[28,29] Herein, we report a simple and convenient nondestructive modification of SWNTs using 1,3-dipoar cycloaddition of pyridinium ylides, readily prepared from simple Kröhnke salts. X-ray photoelectron spectroscopy (XPS), thermogravimetric analysis−mass spectrometry (TGA−MS), atomic force microscopy (AFM), UV−vis-NIR, FTIR and Raman spectroscopy have been employed to characterize the functionalized material.

Experimental Section

Material Preparation. SWNTs. Purified SWNTs produced by the HiPco method and supplied by Unidym, USA, were further purified by heating in air at 400 °C, then soaking in 6 M HCl overnight, followed by filtration over a polycarbonate membrane (0.2 μm), and washing with copious amounts of high-purity water until pH-neutral. The purified SWNTs were annealed under vacuum (10^{-2} mbar) at 900 °C to remove residual carboxylic acid functional groups and any adsorbed gases or solvents.

***N*-(Ethoxycarbonylmethyl)-pyridinium Bromide (1).** The pyridinium salt (1) was prepared following a modified literature procedure.[30] Pyridine (100 mmol) was added to ethyl 2-bromoacetate (110 mmol) and the mixture stirred for 12 h at room temperature. The resulting off-white solid was washed with diethyl ether (3 × 20 mL) to remove excess pyridine and ethyl 2-bromoacetate to afford the pyridinium bromide salt **(1)** (22.64 g, 92%) as confirmed by ^{1}H and ^{13}C NMR and mass spectrometry.

SWNT-Indolizine (Conventional Heating) (2a). SWNTs (10 mg) were dispersed in *N*,*N*-dimethylformamide (15 mL) using mild sonication in an ultrasonic bath (Ultrawave U50, 30−40 kHz) for 5 min and the dispersion heated to 140 °C. The pyridinium salt (1) (1.026 g, 4.17 mmol) was then added to the dispersion followed by triethylamine (0.58 mL, 4.17 mmol) after 30 min. The reaction mixture was refluxed for 5 days, and the functionalized SWNTs were collected via filtration through a PTFE membrane (0.2 μm). The solid SWNTs were then transferred to a cellulose thimble, and impurities and unreacted reagents were removed by Soxhlet extraction using acetonitrile for 18 h. The SWNTs were then dispersed in deionized water (50 mL) and filtered through a PTFE membrane (0.2 μm), dispersed in acetone (50 mL) and filtered through a PTFE membrane (0.2 μm), and finally dispersed in ethanol (50 mL) and filtered through a PTFE membrane (0.2 μm) and dried overnight at 120 °C to afford SWNT-indolizine (**2a**).

SWNT-Indolizine (Microwave Heating) (2b). Using a method similar to that described above, SWNTs (10 mg) were dispersed in *N*,*N*-dimethylformamide (15 mL) using mild sonication in an ultrasonic bath (Ultrawave U50, 30 − 40 kHz) for 5 min. The pyridinium salt **(1)** (1.026 g, 4.17 mmol) and triethylamine (0.58 mL, 4.177 mmol) was then added to the dispersion. The reaction mixture was then heated to 150 °C at 2 bar pressure, in a heat and pressure resistant vessel, with microwaves for 1 h (150 W for 5 min followed by 20 W for 50 min at 2.54 GHz) using a Biotage Initiator Sixty. The SWNTs were washed and isolated as described above to afford SWNT-indolizine (**2b**).

Characterization. AFM. Samples for AFM analysis were produced by drop deposition onto freshly cleaved mica of the corresponding solution of SWNTs (~0.005 mg mL^{-1}) in *N*,*N*-dimethylformamide produced by sonication in an ultrasonic bath (Ultrawave U50, 30−40 kHz) for 15 min. Samples were dried in air before imaging in tapping mode using a Digital Instruments Multimode AFM with a Nanoscope IV controller.

XPS. XPS studies were performed at NCESS, Daresbury laboratory using a Scienta ESCA 300 hemispherical analyzer with a base pressure under 3×10^{-9} mbar. The analysis chamber was equipped with a monochromated Al Kα X-ray source ($h\nu = 1486.6$ eV). Charge compensation was achieved (if required) by supplying low energy (<3 eV) electrons to the samples. XPS data were referenced with respect to the corresponding C 1s binding energy of 284.5 eV which is typical for carbon nanotubes.[17] Photoelectrons were collected at a 45° takeoff angle, and the analyzer pass energy was set to 150 eV giving an overall energy resolution of 0.4 eV.

TGA−MS. Thermogravimetric analysis−mass spectrometry (TGA−MS) data were recorded on 1−3 mg of sample using a Perkin−Elmer Pyris I coupled to a Hiden HPR20 mass spectrometer. Data were recorded in flowing He (20 mL min^{-1}) at a ramp rate of 10 °C min^{-1} to 900 °C after being held at 120 °C for 30 min to remove any residual solvent.

UV−vis-NIR Spectroscopy. The UV−vis-NIR absorption spectra were recorded on a Perkin−Elmer Lambda 900 spectrometer. The samples were prepared by dispersing the nanotube material in *N*,*N*-dimethylformamide (~0.03 mg mL^{-1}) by sonication in an ultrasonic bath (Ultrawave U50, 30−40 kHz) for 5 min followed by filtration through a plug of cotton wool to remove particulates after allowing the solution to stand for 2 h.

Raman Spectroscopy. Raman spectra were recorded using a Jobin Yvon Horiba LabRAM spectrometer in a back scattered confocal configuration using He/Ne (632.8 nm, 1.96 eV), Nd:YAG (532 nm, 2.33 eV) or diode (785 nm, 1.58 ev) laser excitation. All spectra were recorded on solid samples over several regions and were referenced to the silicon line at 520 cm^{-1}.

FTIR Spectroscopy. Infrared spectra were recorded on thick films using a Perkin−Elmer Spectrum 100 equipped with a Pike ATR fitted with a Ge crystal.

Fluorescence Spectroscopy. Fluorescence spectra were recorded on a Perkin−Elmer LS55 luminescence spectrometer using an excitiation wavelength of 335 nm. Samples were prepared by dispersing SWNTs in *N*,*N*-dimethylformamide (0.1 mg mL^{-1}), and allowing them to settle for 8 h followed by filtration.

Results and Discussion

Purified SWNTs were reacted with pyridinium ylides generated in situ by the addition of base to the Kröhnke salt *N*-(ethoxycarbonylmethyl)-pyridinium bromide **(1)** to afford SWNTs with indolizine groups covalently bound to the nanotube surface **(2)**, Scheme 1. The reaction can be carried out using both conventional **(2a)** and microwave heating **(2b)** with the later resulting in significantly shorter reaction times (5 days versus 1 h). The use of microwaves to accelerate cyloaddition reactions on a carbon nanotube surface was recently reported for the cycloaddition of aziridines.[21] The 1,3-dipolar cycloaddition of the pyridinium ylide, to the SWNT surface, with the

(22) Pantarotto, D.; Briand, J.-P.; Prato, M.; Bianco, A. *Chem. Commun.* **2004**, 16.
(23) Kostarelos, K.; Lacerda, L.; Pastorin, G.; Wu, W.; Wieckowski, S.; Luangsivilay, J.; Godefroy, S.; Pantarotto, D.; Briand, J.-P.; Muller, S.; Prato, M.; Bianco, A. *Nat. Nanotechnol.* **2007**, *2*, 108, and references therein.
(24) Mawhinney, D. B.; Naumenko, V.; Kuznetsova, A.; Yates, J. T., Jr.; Liu, J.; Smalley, R. E. *J. Am. Chem. Soc.* **2000**, *122*, 2383.
(25) Banerjee, S.; Wong, S. S. *J. Phys. Chem. B* **2002**, *106*, 12144.
(26) Alvaro, M.; Atienzar, P.; de la Cruz, P.; Delgado, J. L.; Garcia, H.; Langa, F. *J. Phys. Chem. B* **2004**, *108*, 12691.
(27) Alvaro, M.; Atienzar, P.; de la Cruz, P.; Delgado, J. L.; Troiani, V.; Garcia, H.; Langa, F.; Palkar, A.; Echegoyen, L. *J. Am. Chem. Soc.* **2006**, *128*, 6626.
(28) Chen, J.; Hamon, M. A.; Hu, H.; Chen, Y.; Rao, A. M.; Eklund, P. C.; Haddon, R. C. *Science* **1998**, *282*, 95.
(29) Kamaras, K.; Itkis, M. E.; Hu, H.; Zhao, B.; Haddon, R. C. *Science* **2003**, *301*, 1501.
(30) Henrick, C. A.; Ritchie, E.; Taylor, W. C. *Aust. J. Chem.* **1967**, *20*, 2441.

Scheme 1. Schematic Representation of the 1,3-Dipolar Cycloaddition of a Pyridinium Ylide to SWNTs to form an Indolizine

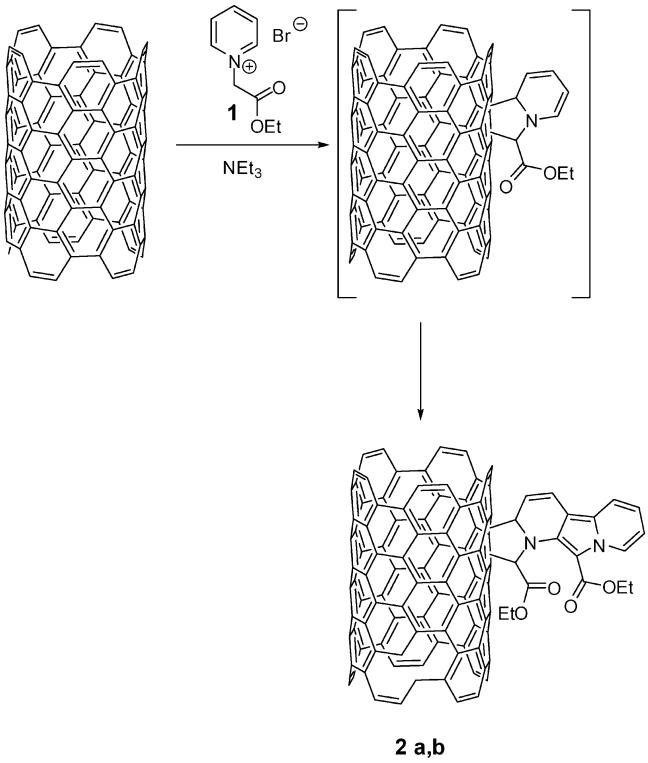

nanotube acting as the dipolarphile, is believed to occur with the pyridinium ylide first adding to the nanotube surface to form a pyrrolidine ring, closely followed by the addition of a second ylide to the addendum on the nanotube surface to afford an indolizine, Scheme 1. The driving force for the double addition of the ylide is likely to be aromatization of the resulting indolizine formed. A similar result occurs in the absence of SWNTs with the pyridinium ylide generated from **(1)** undergoing a 1,3-dipolar cycloaddition with a second pyridinium ylide as evidenced by electrospray mass spectrometry (see Figure S1, in Supporting Information). Indolizine derivatives are particularly interesting as they are well-known for exhibiting a variety of pharmacologically desirable properties, including cardiovascular, anti-inflammatory, and antioxidant properties,[31] as well as having known fluorescent properties and being used in sensor applications.[32,33]

FTIR of the indolizine functionalized SWNTs **(2a)** and **(2b)**, Figure 1, shows the presence of the ester group ($\nu_{(CO)}$ 1730 cm^{-1}) and two bands characteristic of an indolizine at 1632 and 1541 cm^{-1}.[34] The UV−vis-NIR spectra of **(2a)** and **(2b)** are shown in Figure 2, the characteristic features due to the van Hove singularities are clearly present but are suppressed, as expected, when compared to purified SWNTs indicative of chemically modified nanotubes.[13,35−37] The degree of functionalization was probed by gravimetric analysis. TGA−MS of **(2a)** and **(2b)** show a weight loss of 17 and 22%, respectively, at

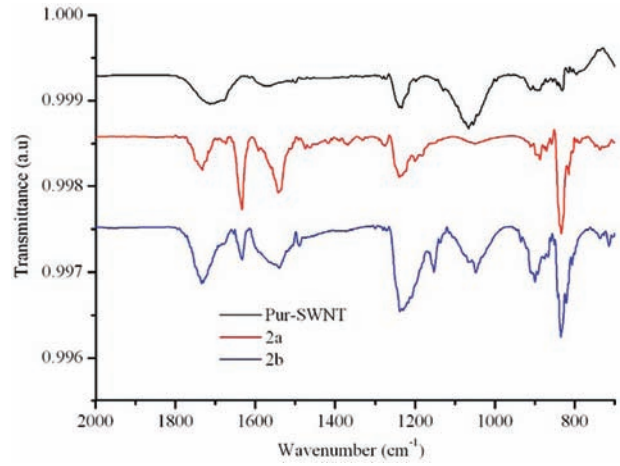

Figure 1. FTIR spectra of purified SWNTs (black), indolizine functionalized SWNTs (**2a**) prepared by conventional heating (red) and indolizine functionalized SWNTs (**2b**) prepared by microwave heating (blue).

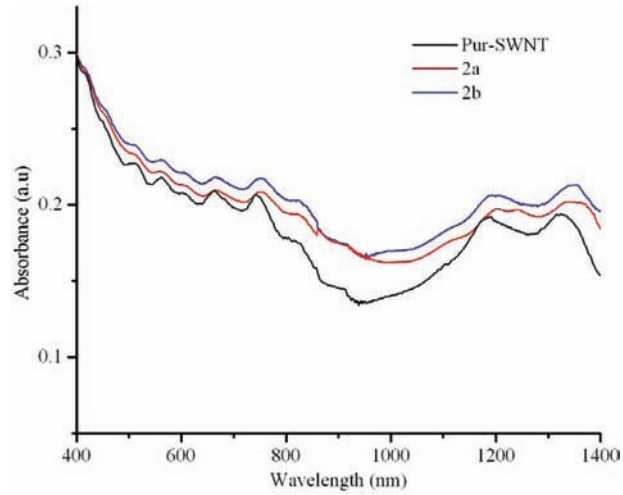

Figure 2. Normalized (at 400 nm) UV−vis-NIR spectra, recorded in *N*,*N*-dimethylformamide, of purified SWNTs (black), indolizine functionalized SWNTs **(2a)** prepared by conventional heating (red) and indolizine functionalized SWNTs **(2b)** prepared by microwave heating (blue).

600 °C compared to ∼7% for purified SWNTs, Figure 3. This corresponds to the presence of ∼1 functional group for every 133 and 96 carbon atoms, respectively. The microwave conditions giving slightly higher levels of functionalization. The peak of mass loss is ∼300 °C, where, although the parent ion of the indolizine is not observed, fragments relating to the ethyl ester group (OEt, 45 amu) and *N*-methylpyridinium (94 amu) were detected by mass spectrometry. Further support and quantification of the level of functionalization is provided by XPS. Measurements, Figure 4, show the presence of a N 1s peak at a binding energy of 398.7 eV characteristic of sp^2 nitrogen.[38] Elemental composition analysis shows the presence of ∼2 atomic percent (at.%) of nitrogen in the sample which is

(31) Gundersen, L.-L.; Malterud, K. E.; Negussie, A. H.; Rise, F.; Teklu, S.; Ostby, O. B. *Bioorgan. Med. Chem.* **2003**, *11*, 5409.
(32) Becuwe, M.; Landy, D.; Delattre, F.; Cazier, F.; Fourmentin, S. *Sensors* **2008**, *8*, 3689.
(33) Sonnenschein, H.; Hennrich, G.; Resch-Genger, U.; Schulz, B. *Dyes Pigm.* **2000**, *46*, 23.
(34) Padwa, A.; Austin, D. J.; Precedo, L.; Zhi, L. *J. Org. Chem.* **1993**, *58*, 1144.
(35) Boul, P. J.; Liu, J.; Mickelson, E. T.; Huffman, C. B.; Ericson, L. M.; Chiang, I. W.; Smith, K. A.; Colbert, D. T.; Hauge, R. H.; Margrave, J. L.; Smalley, R. E. *Chem. Phys. Lett.* **1999**, *310*, 367.
(36) Kazaoui, S.; Minami, N.; Jacquemin, R.; Kataura, H.; Achiba, Y. *Phys. Rev. B* **1999**, *60*, 13339.
(37) Kazaoui, S.; Minami, N.; Kataura, H.; Achiba, Y. *Synth. Met.* **2001**, *121*, 1201.
(38) Camalli, M.; Caruso, F.; Mattogno, G.; Rivarola, E. *Inorg. Chim. Acta* **1990**, *170*, 225.

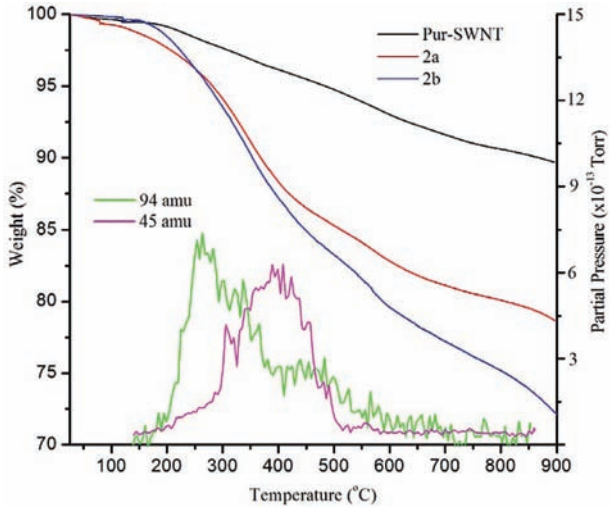

Figure 3. TGA−MS data (10 °C min^{-1}) of purified SWNTs (black), indolizine functionalized SWNTs **(2a)** prepared by conventional heating (red) and indolizine functionalized SWNTs **(2b)** prepared by microwave heating (blue). MS trace (green) of *N*-methylpyridinium (94 amu) and (magenta) ethyl ester fragment (OEt, 45 amu) given off during heating.

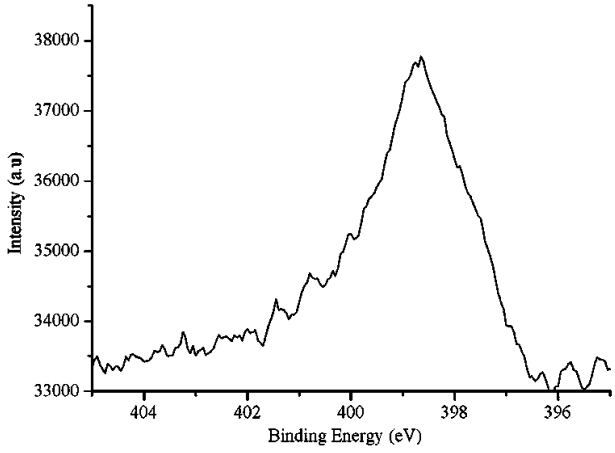

Figure 4. N1s photoelectron spectrum of indolizine functionalized SWNTs **(2b)** prepared by microwave heating.

equivalent to approximately one indolizine group per 83 CNT carbon atoms and is in close agreement with the values determined by TGA−MS.

Given that the fluorescent properties of indolizines are well-known,[32,33] it is perhaps no surprise that the indolizine functionalized SWNTs **(2a)** and **(2b)** emit light upon excitation, Figure 5. Excitation of **(2a)** and **(2b)** at 335 nm results in a blue emission at 416 nm. Unfortunately, quantum yields were not determined due to the strong scattering and absorption of the SWNTs, which made it difficult to compare absolute emission intensities and true quantum efficiencies. However, it was possible to optically image the functionalized SWNTs as a solid material using epi-fluorescence microscopy (See Figure S2 of the Supporting Information), suggesting that the quantum efficiency is sufficiently high for practical applications such as monitoring transfection into cells. Control experiments mechanically mixing the free indolizine, prepared via the 1,3-dipolar addition of the pyridinium ylide to a second pyridinium ylide, with purified SWNTs followed by washing with water and acetone, showed no sign of fluorescence.

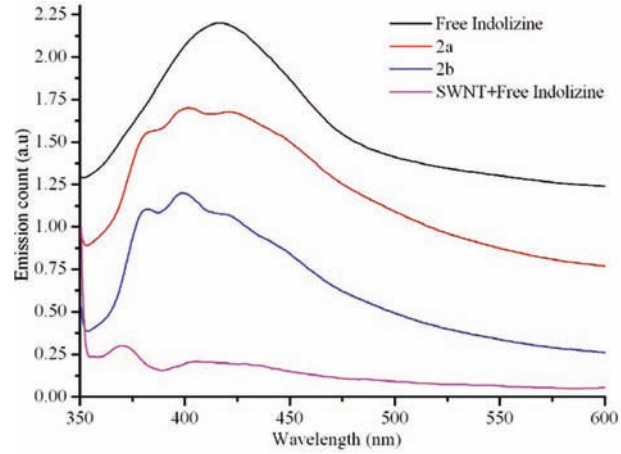

Figure 5. Normalized and offset fluorescence spectra of the indolizine formed from the 1,3-dipolar cycloaddition of the pyridinium ylide, generated from the pyridinium salt **(1)**, with a second pyridinium ylide in the absence of SWNTs (black), indolizine functionalized SWNTs **(2a)** prepared by conventional heating (red), indolizine functionalized SWNTs **(2b)** prepared by microwave heating (blue) and the control experiment of mechanically mixing purified SWNTs with the indolizine generated from the cycloaddition of one pyridinium ylide to another (magenta).

Resonance Raman spectroscopy has been used extensively to study SWNTs.[39−44] A wealth of information regarding the nanotube chirality, electronic type and degree of chemical functional groups (or defects) present can be obtained. A typical Raman spectrum of SWNTs can be divided into four regions; the RBM (radial breathing mode) typically 100−400 cm^{-1}, the disorder or D band from 1280−1320 cm^{-1}, the graphene or G band (tangential mode) 1500−1600 cm^{-1} and the G′ (or D*) band ∼2600 cm^{-1}. The RBM is inversely proportional to the diameter of the nanotube [$\omega_{RBM} = A + (B/d_t)$, where $A = 223.5$ nm cm^{-1}, $B = 12.5$ cm^{-1}, and d_t is the nanotube diameter in nm] which in turn can be related to the chirality of the SWNT as $d_t = (a\sqrt{(n^2 + m^2 + nm)})/\pi$, where n and m are the chiral integers and a is the lattice vector of graphene ($= d_{(c\text{-}c)}\sqrt{3}$, where $d_{(c\text{-}c)}$ is the C−C bond length in nm). The D band is dispersive (shifts to higher frequency as the excitation energy increases) and is linked to the reduction in symmetry of the SWNTs as result of functionalization or the presence of defects, and the ratio of this band with the tangential band (G) is widely used to assess the degree chemical modification in SWNTs.[13,35−37] The tangential mode can be split into two components ω^+_G and ω^-_G associated with vibrations along the nanotube axis and vibrations perpendicular to the nanotube axis, respectively.[45] The G′ (or D*) band is a two-phonon second order Raman scattering process that is pressure dependent and has been used to monitor stress transfer in carbon nanotube composites.[46] The Raman spectra (excited at 632.8 nm and normal-

(39) Strano, M. S. *J. Am. Chem. Soc.* **2003**, *125*, 16148.
(40) Nair, N.; Kim, W.-J.; Usrey, M. L.; Strano, M. S. *J. Am. Chem. Soc.* **2007**, *129*, 3946.
(41) Dyke, C. A.; Stewart, M. P.; Tour, J. M. *J. Am. Chem. Soc.* **2005**, *127*, 4497.
(42) Chattopadhyay, D.; Galeska, I.; Papadimitrakopoulos, F. *J. Am. Chem. Soc.* **2003**, *125*, 3370.
(43) Wunderlich, D.; Hauke, F.; Hirsch, A. *J. Mater. Chem.* **2008**, *18*, 1493.
(44) Banerjee, S.; Wong, S. S. *Nano Lett.* **2004**, *4*, 1445.
(45) Brown, S. D. M.; Jorio, A.; Corio, P.; Dresselhaus, M. S.; Dresselhaus, G.; Saito, R.; Kneipp, K. *Phys. Rev. B* **2001**, *63*, 155414.
(46) Cooper, C. A.; Young, R. J.; Halsall, M. *Compos. Part A* **2001**, *32*, 401.

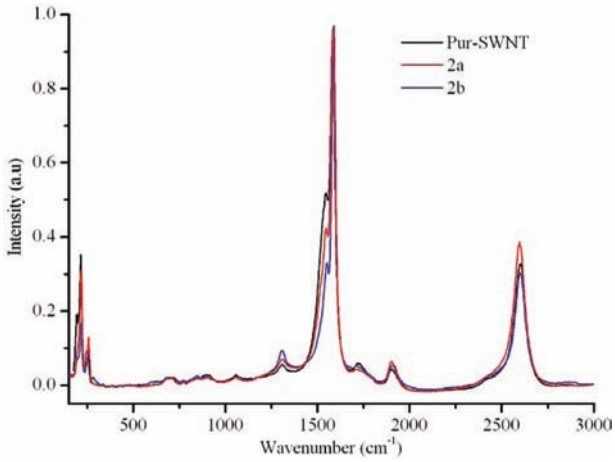

Figure 6. Raman spectra (632.8 nm, 1.96 eV) of purified SWNTs (black), indolizine functionalized SWNTs **(2a)** prepared by conventional heating (red) and indolizine functionalized SWNTs **(2b)** prepared by microwave heating (blue) normalized at the G-band.

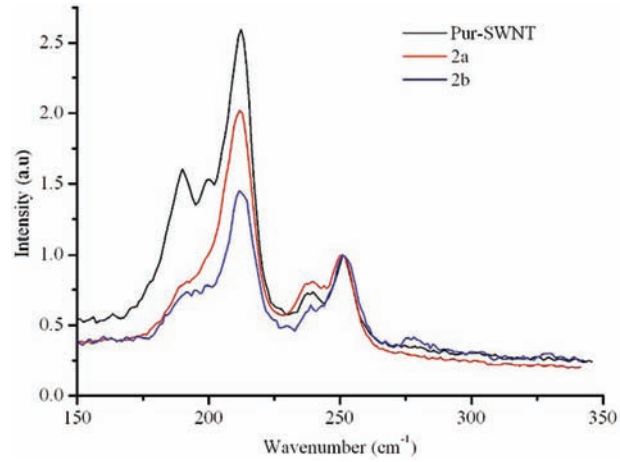

Figure 7. RBM region of the Raman spectra (632.8 nm, 1.96 eV) of purified SWNTs (black), indolizine functionalized SWNTs **(2a)** prepared by conventional heating (red) and indolizine functionalized SWNTs **(2b)** prepared by microwave heating (blue) normalized at 251 cm^{-1}.

ized to the G-band intensity) of pristine SWNTs and the cycloaddition products **(2a)** and **(2b)** are shown in Figure 6. As expected the modified SWNTs **(2a)** and **(2b)** have an enhanced D-band at ~1350 cm^{-1} when compared with unmodified SWNTs, with an I_D/I_G ratio of 0.18 and 0.27, respectively, indicative of groups attached to the surface of the nanotubes.[13,35−37] Close examination of the RBMs in the Raman spectra shows some small differences between the chemically functionalized and pristine SWNTs. From modified Kataura plots,[39] we can establish that excitation at 632.8 nm (1.96 eV) brings into resonance both metallic and semiconducting SWNTs with a diameter range of 0.52 to 1.24 nm, whereas 532 nm (2.33 eV) and 785 nm (1.58 eV) excitation brings into resonance predominately metallic SWNTs (0.84 to 0.99 nm) and semiconducting SWNTs (0.64 to 1.17 nm), respectively, assuming a 50 meV resonance window.[47] Raman spectroscopy at 632.8 nm (1.96 eV), Figure 7, of the unmodified SWNT material in the RBM region shows five peaks at ~187, 197, 209, 236, and 251 cm^{-1}, the latter two being significantly less intense. Using the modified Kataura plots of Strano,[39] these bands are assigned to (12,6), (13,4), (11,5), (12,1), and (10,3) SWNTs, the first three being metallic and the remaining two semiconducting nanotubes. Cycloaddition to form **(2a)** and **(2b)** results in changes in intensity of some of the bands. By normalizing the spectra to the band at 251 cm^{-1} (which is essentially unchanged after reaction), it is clear that the semiconducting SWNTs are relatively unchanged upon functionalization, whereas the bands assigned to metallic SWNTs are significantly reduced in intensity, Figure 7. Excitation at 532 nm (2.33 eV) brings into resonance predominately metallic SWNTs and the spectrum of unmodified SWNTs, Figure 8, shows two bands at 187 and 273 cm^{-1} which can be assigned to (12,6) and (9,3) respectively; the two possible weak bands at 234 and 253 cm^{-1} are ignored. The assignment of the (12,6) SWNTs is tentative, as this nanotube chirality would be expected to be just off resonance using 2.33 eV excitation. Raman spectra,

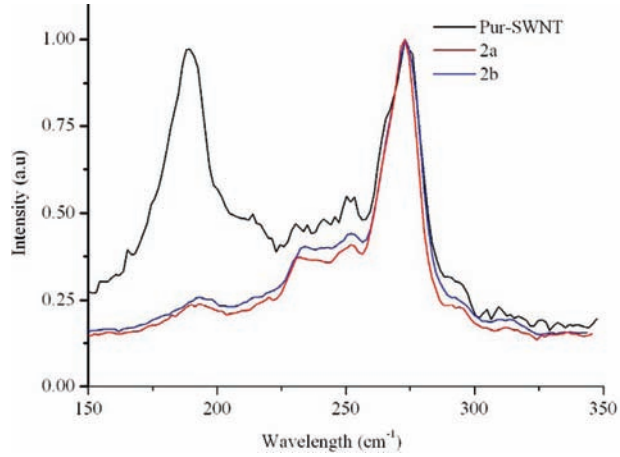

Figure 8. RBM region of the Raman spectra (532 nm, 2.33 eV) of purified SWNTs (black), indolizine functionalized SWNTs **(2a)** prepared by conventional heating (red) and indolizine functionalized SWNTs **(2b)** prepared by microwave heating (blue) normalized at 273 cm^{-1}.

normalized at 273 cm^{-1}, of the functionalized SWNTs (**2a**) and (**2b**), Figure 8, show a significant decrease in the band at 187 cm^{-1} assigned to larger diameter metallic SWNTs. In contrast, excitation at 785 nm (1.58 eV) brings into resonance predominately semiconducting SWNTs and the spectrum of unmodified SWNTs, Figure 9, shows five bands at 202, 212, 222, 230, and 256 cm^{-1} which can be assigned (9,8), (9,7), (10,5), (11,3), and (10,2) respectively; the possible weak band at 245 cm^{-1} is ignored. Note the (10,2) assignment, although the best fit, is tentative, as this nanotube chirality would be just off resonance when excited at 1.58 eV. The Raman spectra of the functionalized SWNTs **(2a)** and **(2b)**, normalized at 265 cm^{-1}, show a significant decrease in the band at 202 cm^{-1} assigned to larger diameter semiconducting SWNTs and a somewhat smaller decrease in the bands at 212, 222, and 230 cm^{-1} attributed to smaller diameter semiconducting SWNTs, Figure 9. The use of resonance Raman for the assessment of selectivity in reactions with SWNTs is particularly useful. As a SWNT becomes functionalized, the electronic properties of the material change and the nanotube moves off resonance, and an apparent decrease in intensity of the normally resonance enhanced RBM is observed.[40−44]

(47) The value of 50 meV for the resonance window was estimated from spectral line widths shown in the following: Bachilo, S. M.; Strano, M. S.; Kittrell, C.; Hauge, R. H.; Smalley, R. E.; Weisman, R. B. *Science* **2002**, *298*, 2361. However, it is noted that a value of 40 meV is stated by Strano in ref 39.

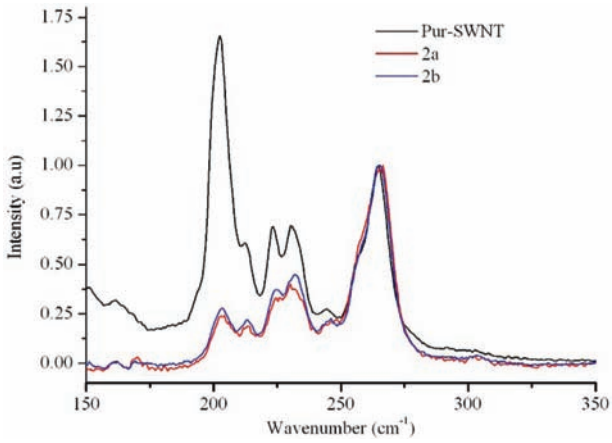

Figure 9. RBM region of the Raman spectra (785 nm, 1.58 eV) of purified SWNTs (black), indolizine functionalized SWNTs **(2a)** prepared by conventional heating (red) and indolizine functionalized SWNTs **(2b)** prepared by microwave heating (blue) normalized at 265 cm^{-1}.

From the results displayed here, it is clear that excitation at 632.8 nm shows that the cycloaddition reaction is selective for metallic SWNTs where 532 excitation shows that selectivity is toward larger diameter metallic SWNTs. Interestingly, 785 nm excitation shows that the reaction is not limited to metallic SWNTs as larger diameter semiconducting SWNTs react. Thus from the resonance Raman data, it is clear that the 1,3-dipolar cycloaddition of pyridinium ylides is selective for metallic and larger diameter semiconducting SWNTs. This is interesting as typically smaller diameter SWNTs are often predicted to be more reactive than their larger counterparts due to the greater degree of curvature and π-orbital misalignment present.[48] However, larger diameter semiconducting SWNTs have been shown to be more reactive than smaller diameter SWNTs to diazonium salts due to the latter having a larger band gap and thus a large region where the density of states (DOS) of the SWNT is zero.[40] The selectivity displayed by the 1,3-dipolar cycloaddition reaction discussed here is similar, metallic more reactive than semiconducting and large diameter semiconducting more reactive than small diameter SWNTs, and thus the reactivity is likely to be correlated with band gap. This fits with a mechanism that first involves electron transfer from the SWNT to the 1,3-dipole, which is in agreement with metallic SWNTs, which have a finite DOS at the Fermi level, being more reactive than semiconducting SWNTs.

Tagging of Functional Groups for AFM Visualization. Definitive characterization of SWNTs functionalized with organic groups using conventional spectroscopy can be difficult and requires extensive use of control experiments to rule out physical adsorption. However, using chemical tagging techniques, we have shown in the past that it is possible to exploit the chemistry of the attached organic group to anchor nanoparticles to the surface of the SWNTs.[15,16] This allows the functional groups to be visualized by atomic force microscopy (AFM) and provides information on distribution and localization of functional groups on the nanotube surface. Here, we have converted the ester group on the indolizine functionalized SWNTs **(2a,b)** to an amide with a terminal tertiary amine, by reaction with *N*,*N*-dimethylethylenediamine, which was subsequently quaternarized by reaction with iodomethane, Scheme 2. The positively charged indolizine functionalized SWNTs were then deposited

Scheme 2. Schematic Representation of the Electrostatic Interaction of Gold Colloids with Indolizine Functionalized SWNTs **(2a,b)** for AFM Functional Group Tagging Experiments[a]

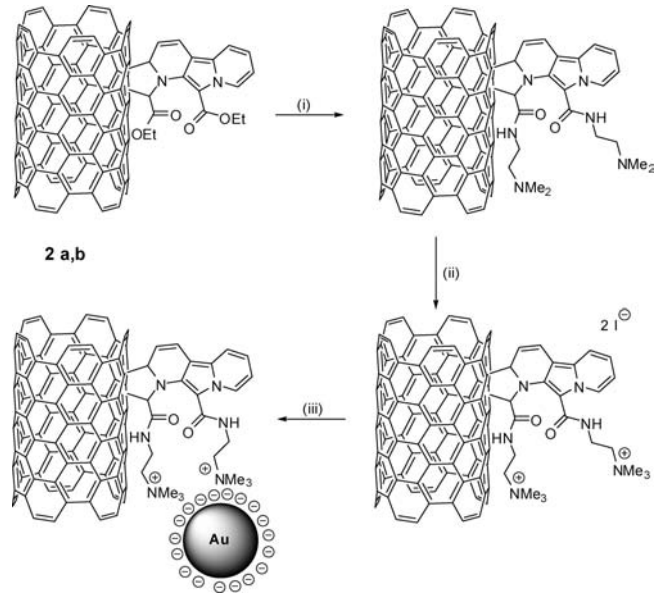

[a] (i) *N*,*N*-Dimethylethylenediamine, 100 °C, 15 h. (ii) MeI, room temperature, 15 h. (iii) Aqueous solution of citrate stabilized gold colloids.

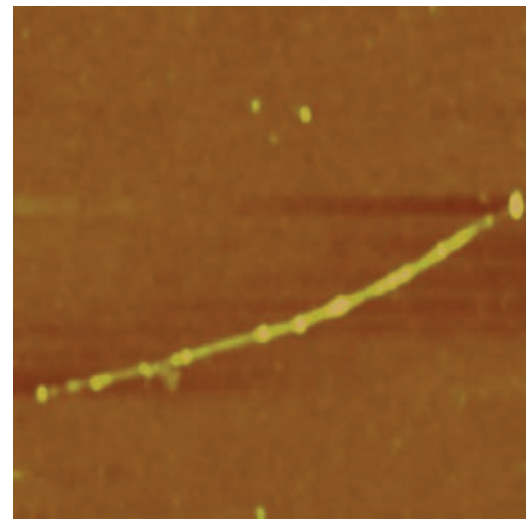

Figure 10. A typical tapping mode AFM height image of an indolizine functionalized SWNT **(2a,b)** with positively charged tertiary amines after exposure to citrate stabilized Au colloids (4−6 nm). The image shown is 1.9 × 1.9 μm with a *z* scale of 0−5 nm. The Au colloids can be seen (light colored features) decorating the complete length of the nanotube.

on a mica surface, where they were exposed to citrate stabilized gold colloids 4−6 nm in diameter, Figure 10. The electrostatic interaction of the negatively charged gold nanoparticles with the positively charge functionalized SWNTs is clear with the gold particles, visible as light features on the AFM height image, showing the presence and distribution of the indolizine functional groups on the nanotube surface.

Conclusions

We have shown that it is possible for SWNTs to undergo 1,3-dipolar cycloaddition, under conventional or microwave

(48) Niyogi, S.; Hamon, M. A.; Hu, H.; Zhao, B.; Bhowmik, P.; Sen, R.; Itkis, M. E.; Haddon, R. C. *Acc. Chem. Res.* **2002**, *35*, 1105.

heating conditions, with pyridinium ylides readily generated from simple and easy to prepare Kröhnke salts. The addition of the pyridinium ylides to the SWNT surface results in the formation of an indolizine group, an important class of compounds that have interesting pharmacological and luminescent properties. The indolizine functionalized SWNTs were shown to emit in the blue (416 nm) when excited at 335 nm. Interestingly, using resonance Raman spectroscopy, we have been able to show that the 1,3-dipolar cylcloaddition to form the indolizines is selective for metallic and large diameter semiconducting SWNTs. This is in agreement with a mechanism first involving donation of electrons from the nanotube to the 1,3-dipole. AFM tagging experiments exploiting the electrostatic interaction of citrate stabilized gold nanoparticles with indolizines that were deliberately positively charged showed that the functional groups were present on the entire length of the carbon nanotubes.

Acknowledgment. We thank Dr. Graham Beamson of the National Centre for Electron Spectroscopy and Surface Analysis (NCESS) at Daresbury Laboratory for technical assistance and useful discussions on the XPS measurements, Doug Carswell for recording the TGA data, and the EPSRC (EP/E025722/1) and TUBITAK (MKB) for funding.

Supporting Information Available: Electrospray mass spectrum of free indolizine prepared from the pyridinium ylide generated from (1) undergoing a 1,3-dipolar cycloaddition with a second pyridinium ylide (Figure S1). Fluorescence image of indolizine functionalized SWNTs Figure S2. This material is available free of charge via the Internet at http://pubs.acs.org.

JA903712F